Electronic Supplementary Information

Efficient Xe selective separation from Xe/Kr/N_2 mixtures over a microporous CALF-20 framework

Yi Wei[1], Fengshi Qi[1], Yunhe Li[1], Xiubo Min[1], Qi wang[1], Jiangliang Hu[2*], Tianjun Sun[1*]

1 Marine Engineering College, Dalian Maritime University, Dalian 116026, China

2 State Key Laboratory of Clean and Efficient Coal Utilization, Taiyuan University of Technology, Taiyuan 030024 China

*Corresponding author: Prof. Dr. Tianjun Sun, E-mail address: suntianjun@dlmu.edu.cn

Contents:

S1. Characterization Details

Powder X-ray diffraction (PXRD) patterns were conducted on an X-ray diffractometer (X-Pert PRO, PANalytical) at 40 kV, 40 mA with Cu-Kαradiation (λ= 0.15406 nm). The XRD patterns were all recorded in the 2θ range of 5-40° with a step size of 0.02° under the scan rate of 8.2°/min at room temperature.

Thermogravimetric analyses (TGA) were performed on a TA analyzer (Labsys Evo, Setaram), in which 3-5 mg samples in alumina pans were heated from 50 ^{o}C to 800 ^{o}C at the rate of 10 $^{o}C \cdot min^{-1}$ under air atmosphere.

Fourier transform infrared (FTIR) spectra were detected on a Nicolet iS50 Fourier transform infrared spectrometer in the range of 4000-400 cm^{-1} at a spectral resolution of 4 cm^{-1} using KBr disks.

Total pore volumes, surface areas, and pore size distribution were measured by nitrogen adsorption-desorption with the Autosorb iQ physical adsorption instrument (Quantachrome Instruments, Boynton Beach, Florida, USA). Prior to the analysis, all samples were degassed at 150 ^{o}C for 2 h under vacuum. Argon adsorption measurements of all MOFs were carried out at 87 K. The argon adsorption isotherms were accurately measured in the pressure range of 0-1 bar, and then a series of textual properties were calculated from these adsorption isotherms. The linearity of fitting for the Brunauer-Emmett-Teller (BET) specific surface area was 0.99999; Total pore volume (V_t) was calculated by Gurvich-rule at P/P_0 =0.95; Micropore volume (V_{mic}) was calculated by t-Plot method; Pore size distribution (PSD) was calculated by the NLDFT method based on a cylindrical pore model since the micropores were dominant in all the samples.

S2. Gas-sorption Measurement Details

Adsorption properties of as-prepared MOFs were characterized by Xe, Kr and N_2

isotherms at 288K, 298 K and 308K in the range of 0-100 kPa, which was conducted on a volumetric gas adsorption instrument Autosorb iQ using typically 1.0 g of sample. All samples were treated under vacuum for 3 h in Autosorb iQ before adsorption measurements. In the measurement of gas adsorption, a Julabo VIVO-RT2 recirculating thermostatic bath was employed to design a water circulating system for maintaining a constant temperature.

All the adsorption data were fitted using the Langmuir-Freundlich (L-F) model:

$$n = n_{max}\frac{b \times p^{1/c}}{1 + b \times p^{1/c}} \tag{S1}$$

where n is the gas capacity, n_{max} is the theoretical maximum gas capacity, p is the gas pressure, b and c are fitting coefficients.

The Henry's law coefficients, H_i, can be calculated from the Langmuir-Freundlich equation as:

$$H_i = n_{max} \times b \tag{S2}$$

Then, Henry's law selectivities for different gas pairs were obtained as:

$$S_{ij} = \frac{H_i}{H_j} \tag{S3}$$

where i and j are the two different gases, H_i and H_j are the corresponding Henry's law coefficient of one pure gas component. At a low partial pressure range, the equilibrium selectivity could be estimated as the ratio of Henry's law constants, which is just the case of xenon capture from dilute sources.

Experimental isosteric heats of adsorption (Qst) of Xe, Kr and N_2 were calculated using Clausius-Clapeyron relation under ideal gas approximation at low temperatures:

$$\ln\frac{P_2}{P_1} = \frac{Q_{st}}{R}\left(\frac{1}{T_1} - \frac{1}{T_2}\right) \tag{S4}$$

Q_{st} is the specific latent heat of the substance; let (P_1T_1) and (P_2T_2) is any two points along the coexistence curve of adsorbate molecules inside the adsorbent between different conditions in general; R is gas constant.

IAST selectivities of different mixtures were estimated and calculated according to the following definition:

$$S = \left[\frac{n_i}{n_j}\right] / \left[\frac{y_i}{y_j}\right] \tag{S5}$$

Where n is the mole amount of gas molecules in the adsorbed phase, and y is the mole fraction of the corresponding gas in the mixture, i and j are the two different gases.

Breakthrough experiments were all carried out in a programmable control system with a thermostat water bath, in which a 250 mm length and 4 mm inner-diameters fixed-bed tube packed with a full volume of 2.2-2.5 g samples was used, as reported in our previous works.[S1] The sample was activated at 372 K for 2 h using helium as a purge gas before each experiment, and then cooled down to room temperature in a temperature-controlled water bath. The breakthrough experiments were performed with the stream of 20 mL/min Xe/Kr and Xe/Kr/N_2 mixtures at 1 bar and 298 K. The composition of the gas outlet was detected by online mass spectrometry (Pfeiffer Vacuum OmniStar GSD 320, Germany), and the whole breakthrough experiment was operated under constant conditions.

S3. Simulation Details

The crystal structures of CALF-20 were taken from the Cambridge Crystallographic Data Centre (CCDC),[S2] and the coordinates of all atoms in CALF-20 were optimized by DFT calculations with the Vienna Ab initio Simulation Package (VASP). The projector augmented wave approximation (PAW) and Perdew-Burke-Ernzerhof (GGA-PBE in VASP) were used for treating the exchange-correlation energy density

functional, in which the weak van der Waals interactions were managed using the dispersion corrections to the total energies through the Grimme's D3 semiempirical method (DFT-D3 in VASP).[S1] For the structure optimization, single-point energy, and related electronic structure calculations, a kinetic energy cutoff of 400 eV was set with the plane wave, and the convergence criteria for the system energy were set to 10-4 eV. Brillouin zone sampling was restricted to the Γ-point. Further geometry optimization of CALF-20 was conducted for obtaining the low-energy structures by the Forcite module in Materials Studio, and Universal Force Field (UFF) was used to account for bonded and non-bonded interactions and the Ewald summation method was utilized for calculating the long-range electrostatic interactions.[S2]

Adsorptions of Xe, Kr and N_2 of these MOFs were carried out at 298 K using Grand Canonical Monte Carlo (GCMC) simulations as implemented in the RASPA code. Peng-Robinson equation of state (PR-EOS) was used to calculate the relationship between the chemical potential and the pressure of the system (fugacites) during the simulation. The simulation box was formed from 2×2×2 unit cells of the optimized lattice structures which were received from the DFT calculations. This structure was used for the simulation, in which all atoms of CALF-20 were maintained fixed and periodic boundary conditions were applied in all dimensions. A cutoff radius of 12.5 Å was adopted for all calculations. Throughout the GCMC simulation, the framework was regarded as a rigid structure and the noble gas atoms could be translated, inserted and deleted randomly. For each simulation, 50000 Monte Carlo cycles were used to guarantee equilibration, followed by additional 200000 production cycles for data collection. A cycle consists of N steps, where N is the maximum of 25 and the number of adsorbate molecules in the supercell which fluctuates during simulation. The interactions for adsorbate-adsorbate and adsorbate-MOF were calculated as the plus of

the Lennard-Jones (LJ) and Coulomb potentials :[S1]

$$v_{ij} = 4\varepsilon_{ij}\left[\left(\frac{\delta_{ij}}{r_{ij}}\right)^{12} - \left(\frac{\delta_{ij}}{r_{ij}}\right)^{6}\right] + \frac{q_i q_j}{4\varepsilon_0 r_{ij}} \quad \text{(S6)}$$

where i and j are interacting atoms, σ_{ij} is the equilibrium diameter at which repulsion occurs, ε_{ij} is the LJ well depth, r_{ij} is the distance between atoms i and j, q_i and q_j are their partial charges, and ε_0 is the dielectric constant. The LJ parameters of the atoms were adopted from the UFF force field and the Metropolis algorithm was used in the calculation. The electrostatic interactions were calculated by the Ewald summation method.[S3]

Results of the adsorption were received as the single-cell adsorption capacity N_{cell}. For comparison with the experimental value, the simulation value should be necessarily converted to the excess adsorption capacity N_{excess} which can be calculated as follows:

$$N_{excess}=N_{absolute}-V_{free}\rho \quad \text{(S7)}$$

Where V_{free} is the free volume of the material which can be calculated as described by Liu,[S1] ρ is the bulk gas density, which is calculated by the PR equation. The calculation method of absolute adsorption amount $N_{absolute}$ is as follows:

$$N_{absolute}=N_{cell}\times 22.4\times 10^3/M_{cell} \quad \text{(S8)}$$

Here, N_{cell} is the adsorption capacity on a single cell, M_{cell} is the relative molecular mass of the cell.

Table S.1. The fitting parameters for the Langmuir-Freundlich equation model of Xe, Kr and N_2 at low pressure and temperature of 298 K on CALF-20 framework

Parameters	CALF-20 @Xe	CALF-20 @Kr	CALF-20 @N_2
n_{max} (mmol·g^{-1})	2.721	3.317	3.774
b (bar^{-1})	8.002	0.498	0.093
c	1.0533	1.0121	1.0237
R^2	0.9991	0.9999	0.9999

Table S.2. Xe adsorption capacity and Xe/Kr selectivity for various MOFs at 298 K and 1 bar.

Adsorbent	Henry's selectivity	Xe uptake (mmol g^{-1})	Reference
MOF-Cu-H	15.8	3.19	26
$Co_3(HCOO)_6$	8.7	2.06	23
Co-Squarate	51.4	1.35	29
NbOFFIVE-2-Cu-i	43.29	3.68	30
Zn-$(tmz)_2$	15.5	3	25
HKUST-1	8.4	3.3	32
SB-MOF-1	16.2	1.4	18
SB-MOF-2	10	2.06	18
MOF-505	6.8	2.2	S4
MOF-74-Co	10.37	6.1	S4,S5
MOF-74-Zn	5.76	3.88	S4,S5
MIL100-Fe	5.6	1.14	22
MIL101-Cr	5.3	1.38	22
UIO-66	6.9	2	22
MOF-801	8.9	1.9	34
Al-Fuma	7.3	3.47	S6
PCN-14	6.5	7.1	33
NOTT-100	6.7	6.1	33
$Zn(ox)_{0.5}(trz)$	12.5	2.54	27
CROFOUR-2-Ni	15.5	1.6	2
PAF-45S	16.7	1.85	28
Al-CDC	10.7	2.45	S7

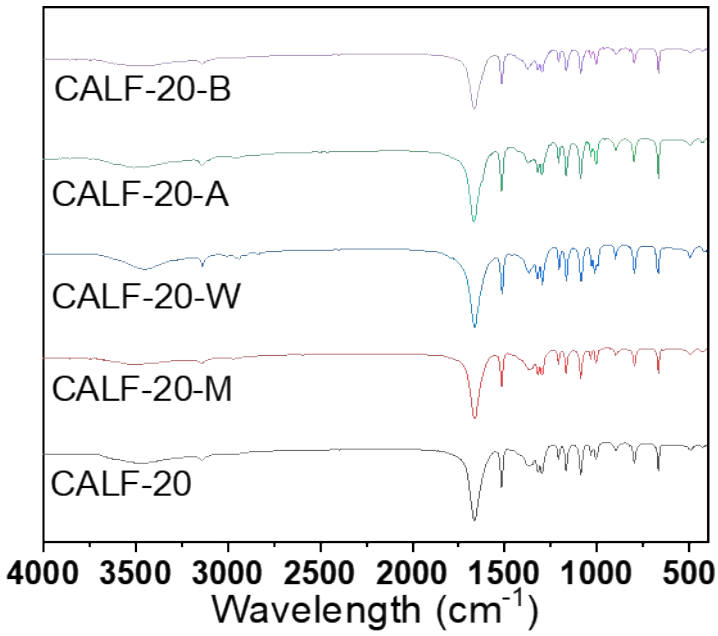

Fig. S.1. FTIR spectra of CALF-20 frameworks treated by different solutions

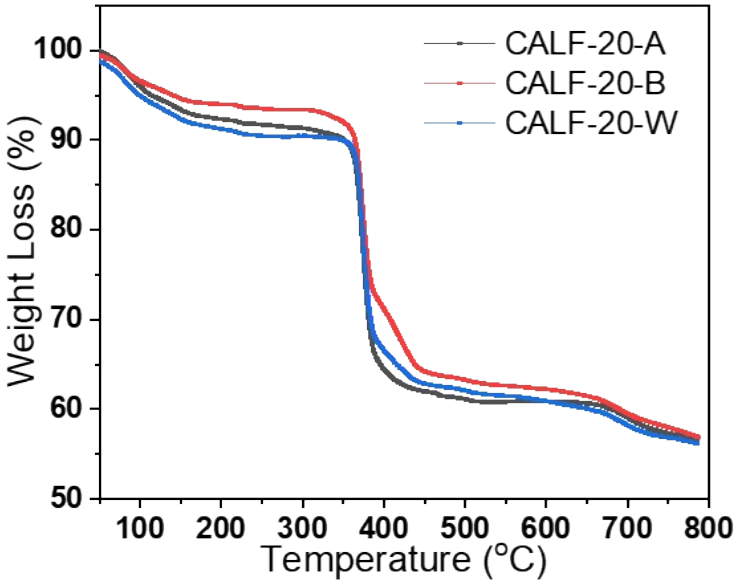

Fig. S.2. TGA curves of CALF-20-A, CALF-20-B and CALF-20-W.

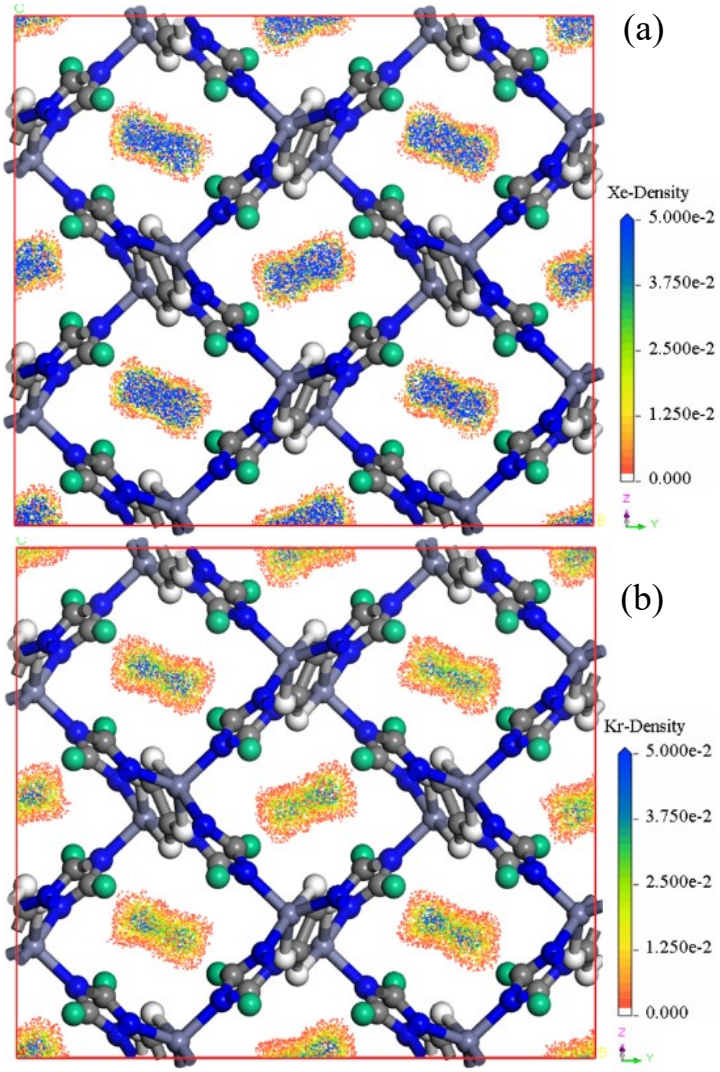

Fig. S.3. Density distribution profiles of Xe **(a)** and Kr **(b)** on CALF-20 frameworks at 100 kPa and 298 K simulated by GCMC method. (Color mode: H, white; O, green; C, gray; N, blue; Zn, indigo blue; Xe, dark green; Kr, golden)

References

S1 X. W. Liu, Y. Guo, A. D. Tao, M. Fischer, T. J. Sun, P. Z. Moghadam, D. Fairen-Jimenez, S. D. Wang, *Chem. Commun.*, 2017, 53, 11437-11440.

S2 P. Z. Moghadam, A. Li, S. B. Wiggin, A. Tao, A. G. P. Maloney, P. A. Wood, S. C. Ward, D. Fairen-Jimenez, *Chem. Mater.*, 2017, 29, 2618-2625.

S3 L. Deliere, S. Topin, B. Coasne, J. Fontaine, S. D. Vito, C. D. Auwer, P. L. Solari, C. Daniel, Y. Schuurman, A. Farrusseng, *J. Phys. Chem. C*, 2014, 118, 25032-25040.

S4 Y. S. Bae, B. G. Hauser, Y. J. Colon, J. T. Hupp, O. K. Farha, R. Q. Snurr, *Micropor. Mesopor. Mat.*, 2013, 169, 176-179.

S5 J. Liu, D. M. Strachan, P. K. Thallapally, *Chem. Comm.*, 2014, 50, 466-468.

S6 Z. T. Yan, Y. J. Gong, C. T. Yang, X. N. Wu, B. Y. Liu, S. S. Xiong, S. M. Peng, *Cryst. Growth Des.*, 2020, 20, 8039-8046.

S7 Z. L. Zhu, B. Li, X. Liu, P. X. Zhang, S. X. Chen, Q. Deng, Z. L. Zeng, J. Wang, S. G. Deng, *Sep. Purif. Technol.*, 2021, 274, 119132.